An Assessment of Turbulence Models for S-Duct Diffusers With Flow Control

Conference Paper · December 2013

DOI: 10.1115/GTINDIA2013-3566

2 authors, including:

Sourabh Pramod Bhat
Indian Institute of Technology Bombay
13 PUBLICATIONS **17** CITATIONS

SEE PROFILE

DRAFT
Proceedings of ASME 2013 Gas Turbine India Conference
GTIndia2013
December 5, 2013, Bangalore, Karnataka, India

GTINDIA2013-3566

AN ASSESSMENT OF TURBULENCE MODELS FOR S-DUCT DIFFUSERS WITH FLOW CONTROL

S. P. Bhat
Assistant Professor
Department of Aerospace Engineering
University of Petroleum & Energy Studies
Dehradun, Uttarakhand, India
spbhat@ddn.upes.ac.in

R. K. Sullerey
Professor (Retired)
Department of Aerospace Engineering
Indian Institute of Technology
Kanpur, India
sullerey@gmail.com

ABSTRACT

The selection of a turbulence model for a problem is not trivial and has to be done systematically after comparison of various models with experimental data. It is a well known fact that there is no such turbulence model which fits all problems ([3], [13]). The flow in S-duct diffuser is a very complex one where both separation and secondary flow coexist. Previous work by the author on CFD analysis of S-duct diffuser was done using k-ε-Standard model [1], however it has been seen that choosing other turbulence model may result in better capturing of the physics in such a problem. Also flow control, to reduce energy losses, is achieved using a technique called Zero Net Mass Flow (ZNMF), in which suction and vortex generation jets (VGJ) are combined and positioned at optimum location. A proper turbulence model has to be chosen for capturing these phenomena effectively. Extensive experimental data is available on this problem and ZNMF technique from previous work done by one of the authors which is used for validating the CFD results. Here the focus is on choosing the best turbulence model for the S-duct diffuser.

Numerical (CFD) analysis is carried out using Ansys Fluent 13.0 with six turbulence models for the geometry with and without flow control and then compared with the experimental results. The turbulence models used are Spalart-Allmaras, three variants of k-ε – Standard, RNG and Realizable and two variants of k-ω – Standard and SST model. All the parameters of comparison are non-dimensionalized using the free stream properties, so that the results are applicable to a wider range of problems. This work is limited to incompressible flow analysis, as the experimental data is only available for low Mach number flows. Comparison of all these models clearly shows that results obtained using k-ω-SST model are very comparable to the experimental results for the bare duct and flow controlled duct both in terms of distribution of properties and aggregate results. Compressible flow analysis can be attempted to achieve reliable results in future with ZNMF using the best turbulence model based on this study.

INTRODUCTION

The problem taken up in this analysis is a diffusing offset duct, with flow control using zero net mass flow (ZNMF) technique which includes suction and active vortex generation simultaneously with the sucked fluid being reused for active vortex generation using vortex generator jets (VGJ), hence the name zero net mass flow. The suction holes and VGJ are positioned and skewed at a optimum location and angle, resulting in a minimum total pressure loss, based on previous experimental study and work done by various researchers([8][9][10][11][12]). However till date, there is no substantial work done in numerical simulation and evaluation of turbulence models for offset diffusing ducts with flow control as per the knowledge of the author. The real application of such a duct would be in the intakes of uninhabited aerial vehicles (UAVs) and combat uninhabited aerial vehicles (UCAVs) where the intakes have sharp bends which are designed from the stealth requirements of hiding the compressor blades of the engine from enemy radar and space constraints. These sharp bends coupled with diffusion results in huge total pressure losses, which can be recovered by avoiding secondary flows. The secondary flows may be reduced by including flow control techniques like ZNMF. The application is generally in the compressible regime, as the Mach number is

greater than 0.3 for such aerial vehicles. This study will therefore feed as an input for numerical analysis of compressible flows in such intake ducts.

It is challenging to determine a suitable turbulence model for a new problem as unreliable results may be obtained with incorrect turbulence model. It is always advisable to validate the model with available experimental results for a similar problem. Before attempting a compressible flow analysis, this study helps in understanding the best turbulence model that will provide reliable results for incompressible flow for such a problem. The turbulence models available in Ansys 13.0 include Spalart-Allmaras, k-epsilon and k-omega (and its sub-types) hence out of the available models the most suitable model is to be chosen. The percentage error in the results is also calculated to assess whether the results are acceptable.

NOMENCLATURE

C_p	Pressure Coefficient $= \frac{(p - p_\infty)(\dot{m}_\infty + \dot{m}_j - \dot{m}_s)}{\frac{1}{2}\rho u_\infty^2 \dot{m}_\infty^2 + \frac{1}{2}\rho u_j^2 \dot{m}_j^2 - \frac{1}{2}\rho u_s^2 \dot{m}_s^2}$
ρ	Density
A	Cross-Sectional Area of the duct
$\infty, 2$	Subscript for inlet and outlet conditions respectively
av	Subscript for average conditions
j	Subscript for jet
s	Subscript for suction
$\dot{m}$	Mass flow rate
u, V, U	Velocity
p_0	Total pressure
ϖ	Mass averaged total pressure loss coefficient $= \frac{(p_{0\infty av} - p_{02av})}{\frac{1}{2}\rho u_\infty^2}$
Re	Reynolds number
X_{ls}	Distance measured along the curved portion of lower or upper wall

DUCT GEOMETRY

The duct being studied is an offset diffusing duct from papers ([1] and [2]) also illustrated in **Figure 1** and a side view of the duct is shown with nomenclature used, in **Figure 2**. The inlet of the duct is of height 72mm and the outlet of the duct is of height 90mm hence resulting in diffusion with an area ratio of 1.25. The offset distance of the centerline of the duct between the inlet and outlet is 31.62 mm. The centerline profile of the duct along the curved geometry is governed by the equations (**1**) – (**4**) with $0 \le \theta \le \theta_{max} = 60°$ and the height of the duct is gradually increased from 72mm to 90mm along the curved length.

For $0 \le \theta \le \frac{\theta_{max}}{2}$:

$$x_c = R\sin(\theta) \quad (1)$$

$$y_c = R\cos(\theta) - R \quad (2)$$

For $\frac{\theta_{max}}{2} \le \theta \le \theta_{max}$:

$$x_c = 2R\sin\left(\frac{\theta_{max}}{2}\right) - R\sin(\theta_{max} - \theta) \quad (3)$$

$$y_c = 2R\cos\left(\frac{\theta_{max}}{2}\right) - R\cos(\theta_{max} - \theta) - R \quad (4)$$

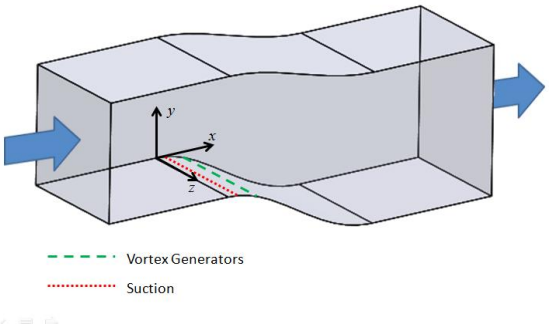

Figure 1: Schematic Duct Geometry

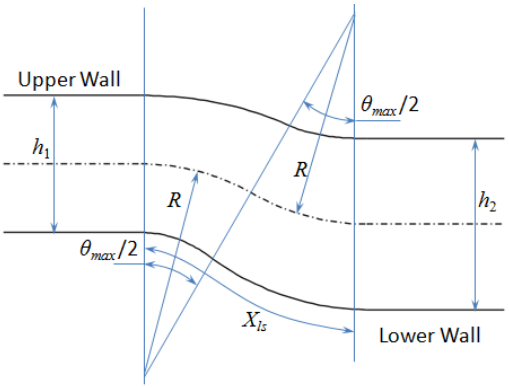

Figure 2: Sketch of Bare Duct Geometry

The width of the duct (along z-axis – see **Figure 1**) is maintained equal to 72mm throughout the length of the duct hence resulting in an inlet cross-section of 72mm x 72mm and an outlet cross-section of 90mm x 72mm. The inlet and outlet of the duct is extended by 80mm, so that the pressure is uniform at the inlet and reattachment of the flow takes place before outlet of the duct. The position of measurement of coefficient of pressure along the lower wall of the duct X_{ls} is normalized (non-dimensionalized) using the total length of the curved lower wall.

The ZNMF duct uses the same geometry used for the bare duct described above with additional suction and VGJ holes on the lower wall of the duct for flow control. There are a total of 23 suction holes of 1.5mm diameter and 4 VGJ holes of diameter 3mm uniformly spaced along the width of the duct. The suction holes are located at 30mm from the start of the

curvature, based on the study by Kerrebrock, et al [8] as it has been seen experimentally that the best flow control is achieved if suction holes are located just upstream of separation. Similarly it has been observed experimentally ([9][10][11][12]), that the best location for VGJ is at the point of maximum pressure difference; hence the VGJ holes are located at 40mm from the start of curvature at maximum secondary flow strength. The VGJ optimized skew angle for the VGJ for this geometry is obtained by Saravana Kumar and R. K. Sullerey [2] to be equal to 60°, based on rigorous experimental study.

GEOMETRY DISCRETIZATION (MESH GENERATION)

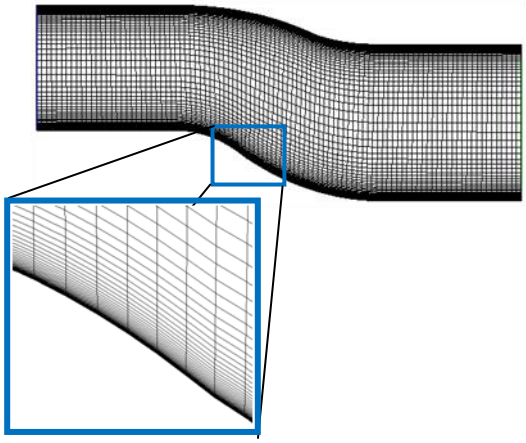

Figure 3: Side View of Mesh for Bare Duct

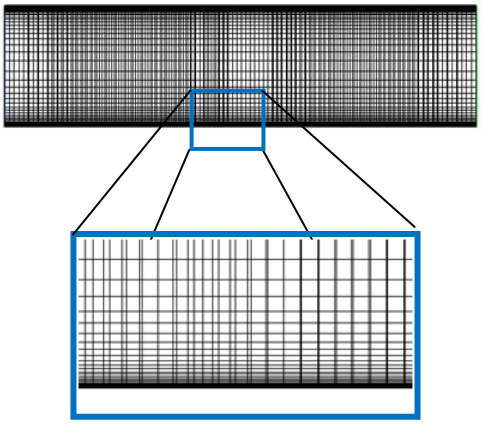

Figure 4: Top View of Mesh for Bare Duct

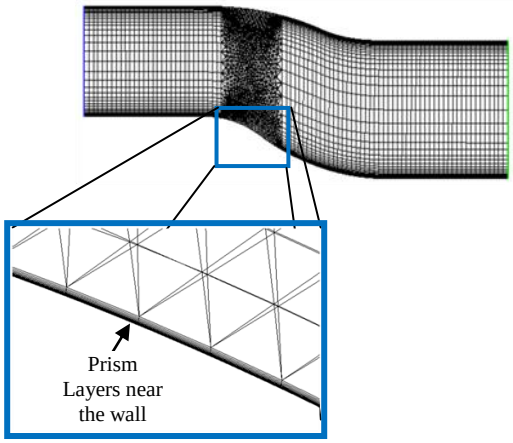

Figure 5: Side View of Mesh for ZNMF Duct

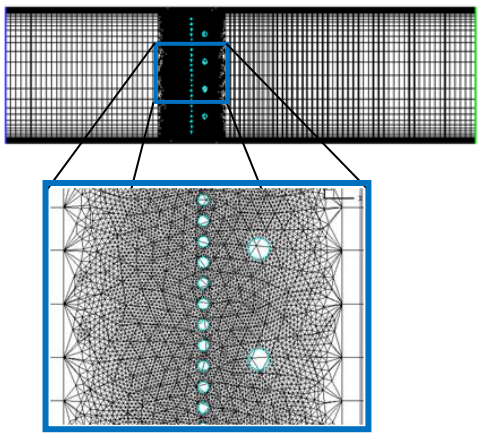

Figure 6: Bottom View of Mesh for ZNMF Duct

For obtaining reliable results numerically it is necessary to have a good mesh with minimum skewed cells, and orientation of the cells in an appropriate direction. The software used for meshing the geometry is Gambit. The bare duct (the duct without flow control) is meshed using structured mesh using hexahedral cells throughout the domain. The orientation of the cells is along the primary flow direction following the shape of the duct as shown in **Figure 3** and **Figure 4**. The ZNMF duct is meshed using the mixed cell types of tetrahedral cells near the suction and VGJ holes and hexahedral cells farther away from the holes in the remaining volume of the duct as shown in **Figure 5** and **Figure 6**. The mixing of cell type helps in capturing the suction and VGJ holes properly, maintaining a less cell count (hence reducing the computational cost) as well as allowing the orientation of cells along the primary flow direction in the majority of the duct volume. The number of

grid cells for the bare duct total to 750,000 and the ZNMF geometry required 1247453 grid cells for adequate spanning of the geometry. The near wall regions use prism layers to capture the high gradients appropriately, which will be resulting due to stationary wall boundary. The first cell height near the wall is calculated based on the curved wall length of the duct, free stream velocity, dynamic viscosity of 1.7894×10^{-5} kg/m-s, density of 1.225 kg/m^3 and using a y^+ of unity. An expansion ratio of 1.2 is used for calculation of subsequent cell heights away from the duct wall. The formula used for calculation of first cell height is given in equation (**5**), (**6**) and (**7**). The value of coefficient of friction C_f is calculated using the empirical relation given in equation (**8**).

$$y = \frac{y^+ \mu}{\rho\, u_*} \tag{5}$$

$$u_* = \sqrt{\frac{\tau_w}{\rho}} \tag{6}$$

$$\tau_w = C_f \frac{1}{2} \rho\, U_\infty^2 \tag{7}$$

$$C_f = [2 \log_{10}(\mathrm{Re}_x) - 0.65]^{-2.3} \quad \text{for } \mathrm{Re}_x < 10^9 \tag{8}$$

SOLVER

The software used for solving the fluid dynamics problem is Fluent 13.0. The parameters in the software are carefully tuned to suit the problem. The solver type used is a density based (coupled), implicit formulation with a Courant number of 5 for bare duct, and a Courant number of 2 for ZNMF duct. Steady state equations are used by progressing to a solution as it converges to a steady state, with residue reducing below 10^{-6} for all the conservation equations and turbulence modeling equations. The solution convergence is also monitored by using drag force as a criterion for convergence, this is done because the pressure distribution is of interest and drag force can be a good indicator to understand that forces have converged. The energy equation is not included i.e. only mass and momentum equations are solved for obtaining results, as temperature variation is not a parameter of interest, and also temperature variations will not be significant for a low subsonic Mach number flow without heat transfer. The fluid is considered to be having a constant density of 1.225 kg/m^3 and a constant viscosity of 1.7894×10^{-5} N-s/m^2, which are the properties of air at sea level at 15°C. The complete flow domain is initialized using the velocity inlet condition i.e. 20m/s and 1% turbulence intensity.

4.1. Boundary Conditions

The bare duct problem is specified in the solver by specifying velocity inlet, pressure outlet and stationary wall boundary conditions. The ZNMF problem uses in addition outlet vent and mass flow inlet boundary condition to specify the suction and VGJ respectively. The boundary conditions are described in detail below:

Velocity inlet: The smaller cross-section boundary has a velocity of 20m/s in the normal inward direction with turbulence intensity of 1%.

Pressure outlet: The larger cross-section of the duct is the outlet for the flow which is assumed to be open to the atmosphere; hence the pressure at the outlet is maintained at atmospheric pressure of 101325 Pa.

Stationary wall: All the other 4 boundaries are specified as stationary walls, without any heat transfer (adiabatic wall).

Outlet vent: The suction is defined using outflow boundary condition with 1.3 % of the duct inlet mass flow rate. The mass flow rate is taken from the optimization study done by S Kumar and Sullerey [2], which is calculated as 1.651×10^{-3} kg/s.

Mass flow inlet: The VGJ are defined using inflow boundary condition with 1.3 % of the duct inlet mass flow rate same as suction, as the sucked fluid is reused for VGJ. The orientation of the jets is defined by direction vector oriented at 60° skew angle.

Turbulence Models

The main aim of this study is to narrow-down to suitable turbulence models for the problem by comparing results obtained by using various models with experimental results. The bare duct and the ZNMF duct is analyzed using six turbulence models available in Fluent, namely, Spalart-Allmaras, three variants of k-ε – Standard, RNG and Realizable and two variants of k-ω – Standard and SST model. All other parameters are maintained same and the focus is only on selection of turbulence model.

The number of iterations taken for solving the problem is maximum for Spalart-Allmaras turbulence model, which required approximately 25,000 iterations for the bare duct. In comparison to SA model; k-ω-SST model required about 60% iterations, k-ε-realizable required about 50% iterations, k-ω-standard required about 40% iterations, k-ε-RNG required about 8% iterations and the minimum iterations were only about 6% for k-ε-standard turbulence model to reduce the residue below 10^{-6}. The Courant number is same for all the cases evaluated as discussed in the above section resulting in these number of iterations.

RESULTS AND DISCUSSION

The comparison plot for Cp distribution over the lower wall (along the normalized curved length X_{ls}) of the bare duct using all turbulence models (continuous lines) with experimental results (diamond markers) is shown in **Figure 7** and the comparison plot for Cp distribution over the upper wall of the bare duct using all turbulence models with experimental results is shown in **Figure 8**. It can be seen from the plots that k-ε-Realizable and k-ω-SST models behave very well in

accordance to the experimentally observed Cp distribution. The k-ω-SST model is also able to capture the upstream Cp distribution very close to the experimental observation. The Spalart-Allmaras model on the other hand behaves very poorly as seen from the plots. It can be concluded from these observations that Spalart-Allmaras model (which uses wall-functions) must only be used for course meshes with large y^+, however for fine meshes and small y^+(as considered in this case y^+=1) for offset diffusion ducts k-ω-SST or k-ε-Realizable model has to be used to obtain reliable results.

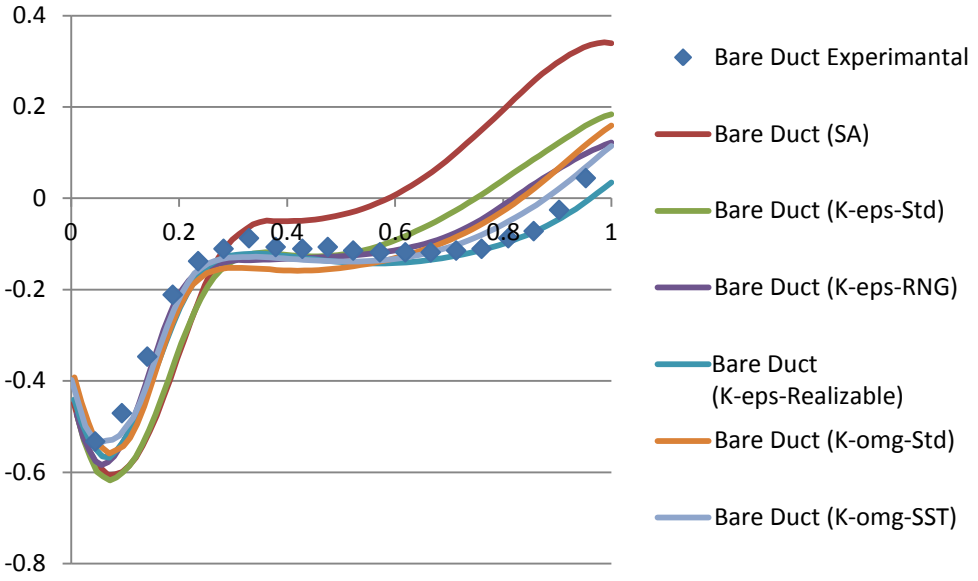

Figure 7: Comparison of Cp distribution at lower wall for bare duct between turbulence models and experimental results

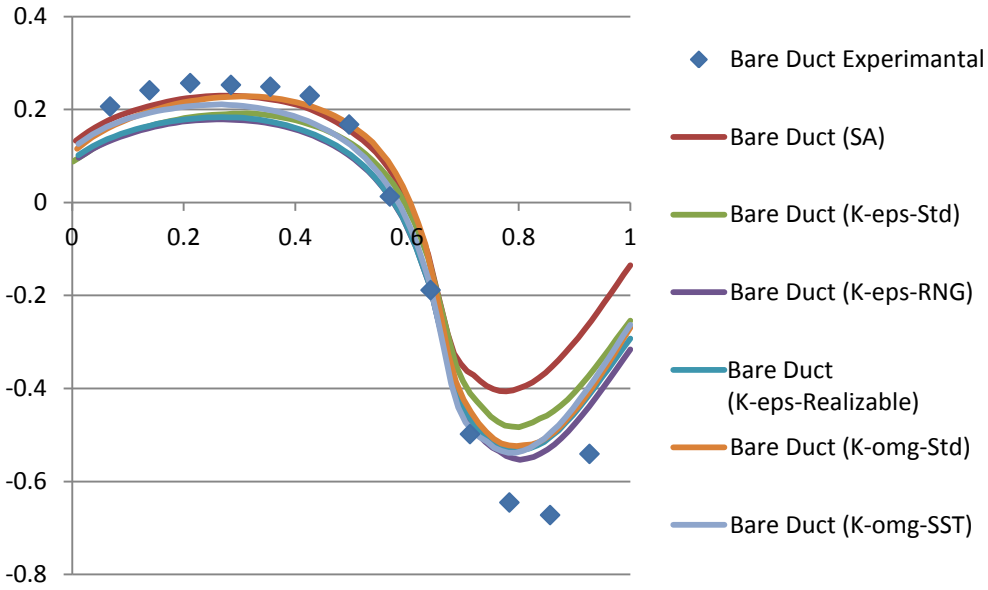

Figure 8: Comparison of Cp distribution at upper wall for bare duct between turbulence models and experimental results

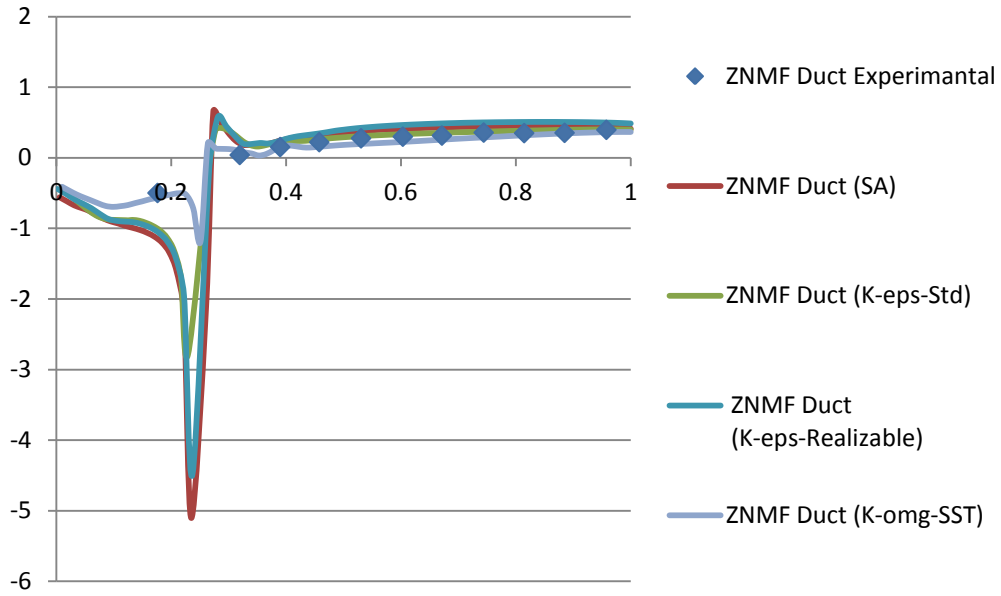

Figure 9: Comparison of Cp distribution at lower wall for ZMNF duct between turbulence models and experimental results

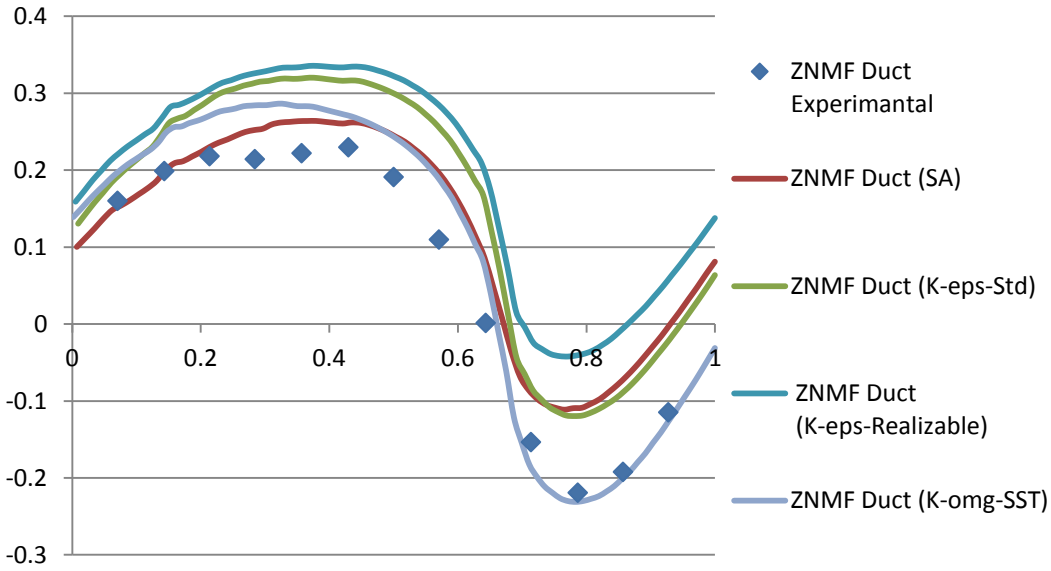

Figure 10: Comparison of Cp distribution at upper wall for ZMNF duct between turbulence models and experimental results

The comparison plot for Cp distribution over the lower wall of the ZNMF duct using all turbulence models with experimental results is shown in **Figure 9**. The sudden dip in Cp plot is due to the points of measurement lying on the suction and VGJ holes and thus may be neglected in the comparison. The comparison plot for Cp distribution over the upper wall of the ZNMF duct using all turbulence models with experimental results is shown in **Figure 10**. It can be seen from the plots that k-omega-SST model compare very well with the experimental results. Other models did not perform very well and hence k-omega-SST model may be used further to study compressible flow.

The comparison of experimentally observed total pressure loss coefficient contours, at the exit plane of the bare duct and ZNMF duct with turbulence models is shown in **Figure 11a** through **Figure 11g** and **Figure 12a** through **Figure 12g** respectively. The experimental observation shows a skew of contours most probably due to unsteady flow or minor non-

symmetry in experimental geometry, however the overall trend of results is similar in experimental and numerical results. For comparison with experimental results and deciding upon the best turbulence model average values as tabulated in **Table 1** are used.

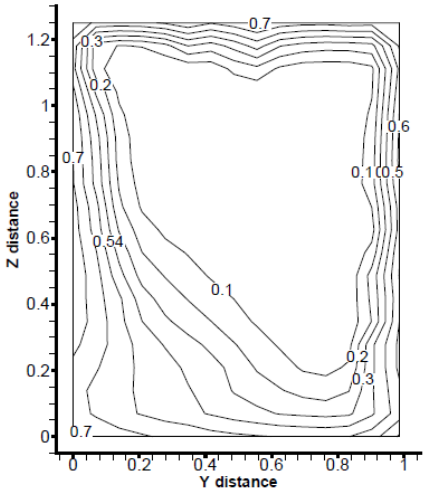

a) Experimental Result

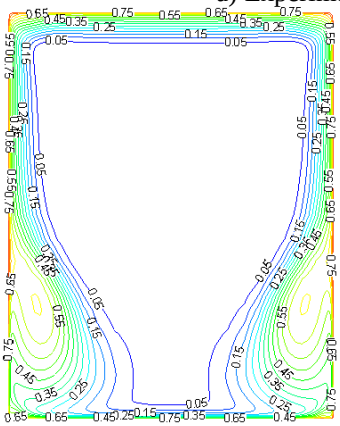

b) Spalart Allmaras

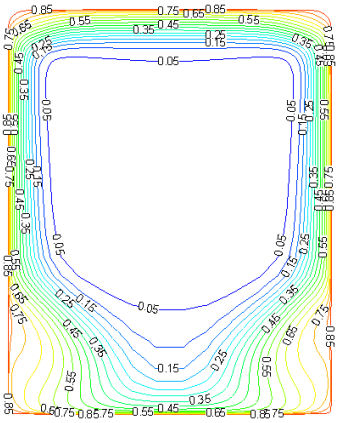

c) k-epsilon-standard

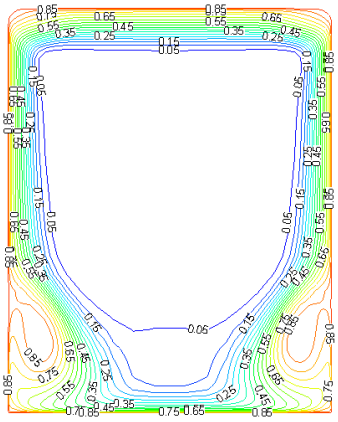

d) k-epsilon-RNG

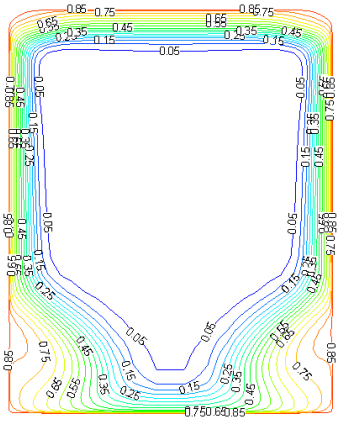

e) k-epsilon-realizable

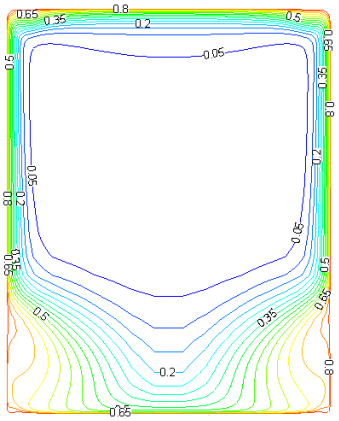

f) k-omega-standard

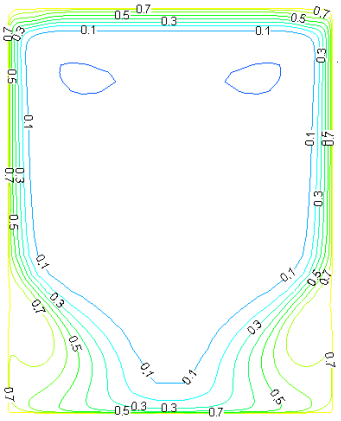

g) k-omega-SST

Figure 11: Contours of total pressure loss coefficient for bare duct

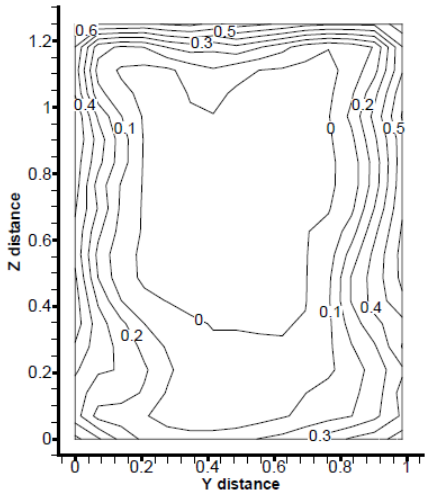

a) Experimental Result

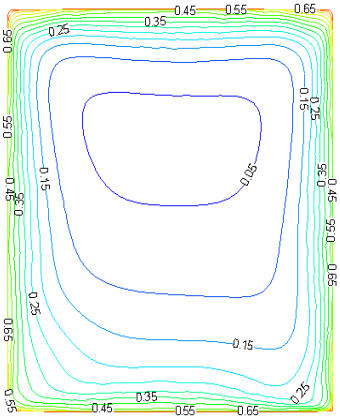

b) Spalart Allmaras

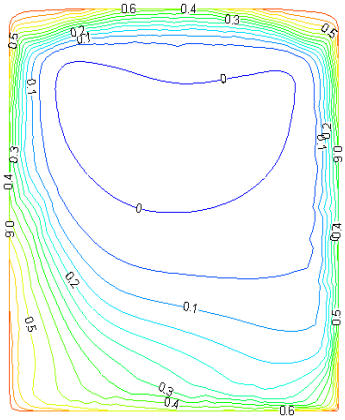

c) k-epsilon-standard

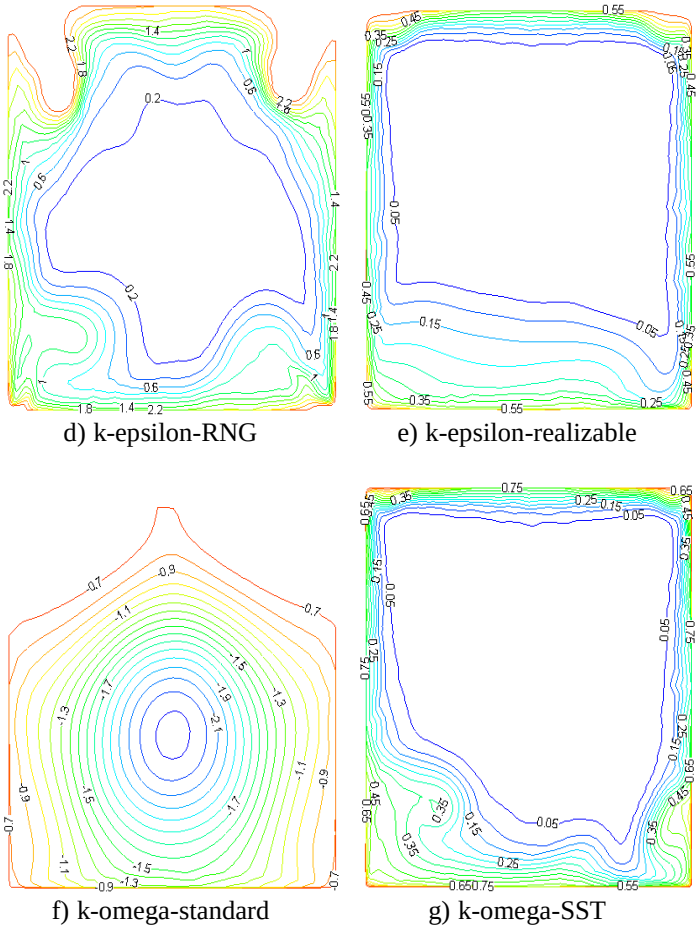

d) k-epsilon-RNG e) k-epsilon-realizable

f) k-omega-standard g) k-omega-SST

Figure 12: Contours of total pressure loss coefficient for ZNMF duct

Table 1 shows the summary of total pressure loss coefficient (ϖ) and associated errors in numerical results (percentage difference in comparison to experimental results) using various turbulence models.

Table 1: Summary of loss coefficients and comparison of numerical results with the experimental resuts

		Bare Duct	ZNMF
		ϖ (% Error)	ϖ (% Error)
Experimental		0.226	0.116
Numerical (Turbulence Models)	SA	0.158 (30.1%)	0.173 (49.1%)
	k-ε-Std	0.234 (3.5%)	0.142 (22.41%)
	k-ε-RNG	0.235 (4.0%)	0.0833 (28.1%)
	k-ε-Realz	0.221 (2.2%)	0.0840 (27.6%)
	k-ω-Std	0.194 (14.2%)	0.180 (55.2%)
	k-ω-SST	0.221 (2.2%)	0.116 (0 %)

The results shown in **Table 1** reinforce the previous observation that the percentage error in calculation of total pressure loss and prediction of pressure distribution is minimum for the k-ω-SST turbulence model and maximum for Spalart-Allmaras turbulence model. It can be clearly seen that k-ω-SST turbulence model behaves the best amongst the compared turbulence models and may be used for compressible flow analysis of similar problems. This model behaves so well for the problem mostly because k-ω-SST turbulence model is based on the combination of k-ε, k-ω turbulence models and also uses wall functions and hence the near wall phenomenon is captured more accurately, thus resulting in a better modeling of separation dominated problems.

CONCLUSION

In this study various turbulence models available in Fluent 13.0 are compared, to assess these turbulence models for their performance in offset and diffusing ducts. The study also includes the behavior of the turbulence models with flow control using ZNMF technique. It has been observed that k-ω-SST turbulence model behaves the best for both with and without flow control. The results obtained are summarized in **Table 1** mainly concentrating on the parameter of interest which is the pressure loss coefficient. The application of such ducts is in UAV and UCAV engine inlets, wherein the flow is at high subsonic speeds, and thus compressibility of the fluid has to be considered in the analysis. The future of this work is therefore to analyze compressible flows using a reliable turbulence model selected based on the results of this study.

REFERENCES

[1] R K Sullerey and S P Bhat (2012), Numerical Analysis Of Flow In S-Duct Diffusers With And Without Flow Control, *Proceedings of ASME 2012 Gas Turbine India Conference*, Maharashtra, India.

[2] S S Kumar (2011), Flow control in S-duct diffuser with Zero-Net-Mass-Flow, *M. Tech. Thesis*, Dept. of Aerospace Engg., Indian Institute of Technology, Kanpur, India.

[3] S M El-Behery and M H Hamed (2011), A comparative study of turbulence models performance for separating flow in a planar asymmetric diffuser, *Computers & Fluids*, 44, pp. 248-257.

[4] R K Sullerey and A M Pradeep (2003), Secondary Flows and Separation in S-Duct Diffusers – Their Detection and Control, *Proc. of FEDSM'03, 4TH ASME/JSME Joint Fluids Engg. Conf.*, Honolulu, Hawaii, USA.

[5] R K Sullerey, S Mishra and A M Pradeep (2002), Application of Boundary Layer Fences and Vortex Generators in Improving the Performance of S-duct Diffusers, *ASME J. Fluids Eng.*, 124, pp. 136-142.

[6] A M Pradeep, R K Sullerey (2006), Active Flow Control in Circular and Transitioning S-Duct Diffusers, *Journal of Fluids Engineering*, Vol. 128, pp. 1192-1203.

[7] R K Sullerey and A M Pradeep (2004), Secondary Flow Control Using Vortex Generator Jets, *ASME Transactions Journal of Fluids Engineering*,Vol. 126, pp.1-8.
[8] J Kerrebrock, et al. (1998), A Family of Designs for Aspirated Compressors, *ASME 98- GT-19*.
[9] R K Sullerey,S Mishra and A M Pradeep (2002), Application of Boundary Layer Fences and Vortex Generators in Improving the Performance of S-duct Diffusers, *ASME J. Fluids Eng.*, 124, pp. 136-142.
[10] J P Johnston and N Michhiro (1990), Vortex Generator Jets-Means for Flow Separation Control, *AIAA Journal*, Vol. 28, No. 6, pp 989-994.
[11] R K Sullerey and A M Pradeep (2003), Secondary Flows and Separation in S-duct Diffusers-Their Detection and Control, *FEDSM2003-45109, Proceedings of the 4th ASME/JSME Joint Fluids Engineering Conference*, Honolulu, Hawaii, USA.
[12] J Foster, B J Wendt, B A Reichert and T H Okiishi (1997), Flow Through a Rectangular-to-Semi-Annular Diffusing Transition Duct, *Journal of Propulsion and Power*, 13, pp. 312-317.
[13] Christopher J. Roy and Frederick G. Blottner, (2006), Review and assessment of turbulence models for hypersonic flows, Progress in Aerospace Sciences, 42, 469–530